# Antiferromagnetic resonance in methylaminated potassium fulleride $(CH_3NH_2)K_3C_{60}$

Denis Arčon
*Institute Jozef Stefan, Jamova 39, 1000 Ljubljana, Slovenia*
*and Faculty of Mathematics and Physics, University of Ljubljana, Jadranska 19, 1000 Ljubljana, Slovenia*

Matej Pregelj and Andrej Zorko
*Institute Jozef Stefan, Jamova 39, 1000 Ljubljana, Slovenia*

Alexey Yu. Ganin and Matthew J. Rosseinsky
*Department of Chemistry, University of Liverpool, Liverpool L69 7ZD, United Kingdom*

Yasuhiro Takabayashi and Kosmas Prassides
*Department of Chemistry, University of Durham, Durham DH1 3LE, United Kingdom*

Hans van Tol and L.-C. Brunel
*National High Magnetic Field Laboratory, Florida State University, Tallahassee, Florida 32310, USA*
(Received 7 May 2007; revised manuscript received 16 August 2007; published 3 January 2008)

High-frequency magnetic resonance measurements ($\nu_L$=9.6–420 GHz) were employed to investigate the low-temperature antiferromagnetic ground state of the $(CH_3NH_2)K_3C_{60}$ fulleride. The frequency and temperature dependence of the intensity, linewidth, and center of the resonance signal detected below $T_N$ are characteristic of antiferromagnetic resonance (AFMR). The AFMR intensity is consistent with an ordered magnetic moment of $\mu_{eff}=0.7(1)\mu_B/C_{60}$, while the narrowing of the AFMR signal with increasing resonance frequency can be modeled with a spin-flop field of $H_{sf}$=840(80) G and a $g$-factor anisotropy of $\delta\gamma$=710(50) ppm. We stress that the spin-flop field is reduced compared to the ammoniated analog $(NH_3)K_3C_{60}$ on the account of reduced $C_{60}^{3-}$-$C_{60}^{3-}$ exchange interactions. Differences in the level of the anisotropic expansion between $CH_3NH_2$ and $NH_3$ cointercalated fullerides are likely to be responsible for the differences in the electronic structure between the two systems and ultimately may account for the reduced Néel temperature in $(CH_3NH_2)K_3C_{60}$.

DOI: 10.1103/PhysRevB.77.035104 PACS number(s): 72.80.Rj, 76.50.+g, 76.60.Jx

## INTRODUCTION

Alkali-doped $C_{60}$ compounds ($A_nC_{60}$, where $A$=alkali metal and $n$=1–6) have emerged in recent years as intriguing "narrow-band" strongly correlated electronic systems in which the important energy scales, such as bandwidth ($W$), on-site Coulomb repulsion ($U$), phonon energies, and Jahn-Teller energies are all of comparable magnitude.[1,2] The bandwidth is very efficiently controlled by the interfullerene separation as the overlap of the $t_{1u}$ wave functions decreases with increasing distance (thereby leading to a decrease in bandwidth). A striking manifestation of this dependence is the monotonic increase of the superconducting transition temperature $T_c$ with increasing cubic unit cell lattice parameter in the $A_3C_{60}$ fullerides.[3,4] As the interfullerene distance increases, the significance of the intrafullerene electron repulsion increases and eventually at large unit cell volumes, the fullerides undergo a metal-to-antiferromagnetic (AFM) insulator transition. This notion proved to work extremely well in ammoniated $A_3C_{60}$ samples, where $NH_3$ cointercalation results in large unit cell expansions. For instance, $(NH_3)K_3C_{60}$ undergoes a transition to a nonmetallic AFM ordered state below $T_N$=40 K.[5–8] High-pressure studies revealed the recovery of superconductivity above ~10 kbar,[9] suggesting that $(NH_3)K_3C_{60}$ is in close proximity to the metal-insulator boundary in the fulleride phase diagram.

Recent attempts toward affording even larger expansions of the fulleride unit cell have successfully led to the isolation of the methylaminated potassium fulleride phase, $(CH_3NH_2)K_3C_{60}$.[10] High-resolution synchrotron x-ray powder diffraction studies are consistent with a face-centered orthorhombic unit cell (space group *Fmmm*) with lattice parameters $a$=15.205 Å, $b$=15.179 Å, and $c$=13.503 Å at room temperature. The large very anisotropic unit cell expansion is responsible for the nonmetallic ground state in analogy with the ammoniated alkali fulleride systems. Moreover, a recent zero-field muon spin relaxation study (ZF-$\mu^+$SR)[11] of $(CH_3NH_2)K_3C_{60}$ revealed the development of magnetic long-range order below ~10 K as evidenced by the appearance of a strongly damped oscillating signal. This work was complemented by a detailed study of the temperature dependence of the $X$-band electron paramagnetic resonance (EPR) response in this fulleride.[12] Compelling evidence for a transition to a long-range-ordered AFM state was provided by the rapid disappearance of the electron paramagnetic resonance signal and the accompanying broadening below $T_N$ =11 K. However, as direct evidence for the development of the antiferromagnetic state in $(CH_3NH_2)K_3C_{60}$ is still lacking, we have now extended our EPR measurements to higher resonance frequencies. We report direct observation of the antiferromagnetic resonance (AFMR) at low temperatures, which provides unambiguous evidence for a transition to a long-range-ordered antiferromagnetic state and completes

 

the picture of $(CH_3NH_2)K_3C_{60}$ as an antiferromagnetic insulator in close correspondence with the properties of ammoniated fullerides. The analogy, however, breaks when one compares the Néel temperatures of $(CH_3NH_2)K_3C_{60}$ and the $NH_3K_{3-x}Rb_xC_{60}$ $(0 \leqslant x \leqslant 3)$ materials with similar unit cell volumes. In $(CH_3NH_2)K_3C_{60}$, $T_N$ is strongly reduced, indicating weakened exchange interactions between $C_{60}^{3-}$ ions at comparable values of the mean interfullerene separation. To rationalize this effect, we discuss the possible influence of the enhanced anisotropic expansion in $(CH_3NH_2)K_3C_{60}$ on its electronic structure, the degree of orbital order, and the reduction of the Néel ordering temperature compared to ammoniated systems.

## EXPERIMENTAL DETAILS

The $(CH_3NH_2)K_3C_{60}$ sample used in the present work was prepared by the reaction of single-phase $K_3C_{60}$ powder with $CH_3NH_2$ vapor, as described before.[10] Phase purity was confirmed by synchrotron x-ray diffraction with the high-resolution powder diffractometer on beamline ID31 at the European Synchrotron Radiation Facility (ESRF), Grenoble, France. Field-modulated continuous wave EPR experiments at frequencies ranging between 24 and 420 GHz were performed at the National High Magnetic Field Laboratory facility, Tallahassee, Florida.[13] A Gunn oscillator[14] was used as a microwave source in the transmission geometry. An Oxford Cryogenics cryostat with temperature stability better than ±0.1 K was used for low-temperature experiments down to 4 K. Complementary *X*-band (9.6 GHz) EPR experiments were conducted with a homebuilt cw spectrometer using a Varian magnet. An ESR900 Oxford Cryogenics cryostat and an ITC503 temperature controller were used for sample cooling with temperature stability better than ±0.1 K over the entire temperature (4–300 K) range.

The resonance signal line shape becomes very broad and asymmetric at very low temperatures and for this reason, we applied the moment analysis. To make the calculation of the second moment stable, we considered in the second moment calculations only those spectral points which are above threshold level (the threshold was set to $\varepsilon=5\%$ of the maximum of the signal). As a consequence of this assumption, the relation between the second moment and the linewidth is not straightforward. For instance, for a Lorentzian line shape, if one take into account only points within the interval $|H-H_C| \leqslant \alpha$, the second moment reads $M_2=2\alpha\delta/\pi$, where $\delta$ is the half width at half maximum.[15] Relating our threshold level $\varepsilon$ to $\alpha$, one can derive the expression for the second moment to be $M_2=(2/\pi)\sqrt{(1-\varepsilon)/\varepsilon}\delta^2$. In our analysis for a Lorentzian line shape, the full width at the half maximum is related to the second moment as $\Delta H=1.2\sqrt{M_2}$.

## THEORETICAL BACKGROUND

In this section, we briefly introduce the basic properties of antiferromagnetic resonance[16] and especially the way it was used to authenticate the electronic ground state in other prototypical antiferromagnetic fullerides.[15–18] Assuming an antiferromagnet in which the axial anisotropy is given by the anisotropy field $H_A$, the two relevant resonance modes for the orientation of the magnetic field perpendicular and parallel to the easy axis are given by

$$\omega_{\pm} = \gamma_{\pm}\sqrt{H_R^2 \pm 2H_E H_A}. \tag{1}$$

Here, $H_R$ is the resonance field, $H_E$ is the exchange field, and $\gamma_{\pm}$ is the gyromagnetic ratio for the given field orientation (parallel and perpendicular to the antiferromagnetic easy axis, respectively). In order to account for the anisotropy, we use the same notation as in Ref. 18 and write $\gamma_{\pm} = \gamma_0\left(1 \pm \frac{1}{2}\delta\gamma\right)$, where $\delta\gamma$ is now a measure of the *g*-factor anisotropy. The relation is valid only for magnetic fields larger than the spin-flop field, $H_{sf}=\sqrt{2H_E H_A}$. In a powdered sample, all crystal orientations with respect to the external magnetic field have to be taken into account and in a field-sweep experiment with a resonance frequency, $\omega_L=2\pi\nu_L$, one expects a resonance signal between the two fields,[18]

$$H_R^{\pm} = \sqrt{\frac{\omega_L^2}{\gamma_{\pm}^2} \mp H_{sf}^2}. \tag{2}$$

The resonance linewidth is then given by $\Delta H=H_R^- - H_R^+$. It is also evident from Eq. (2) that in the high-field expansion limit and for negligible *g*-factor anisotropy, the linewidth $\Delta H$ becomes proportional to $H_E H_A / H_R$, i.e., the linewidth of the signal is predicted to decrease with increasing resonance field. Such a behavior is in striking contrast to that of a paramagnetic EPR signal for which the linewidth increases with increasing frequency in the presence of *g*-factor anisotropy.

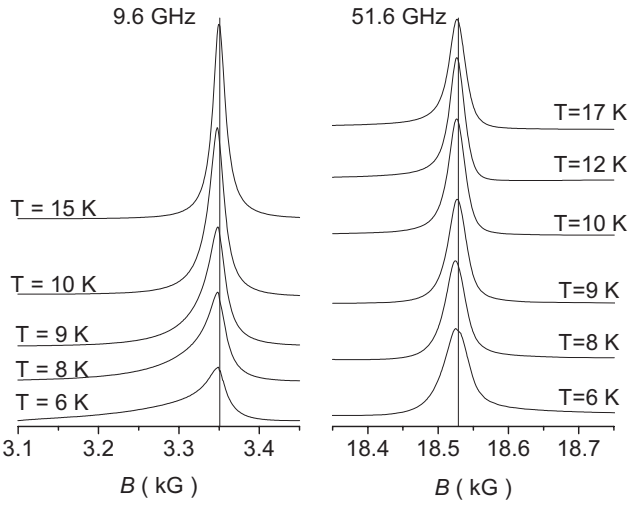


FIG. 1. Temperature dependence of the integrated magnetic resonance spectra of polycrystalline $(CH_3NH_2)K_3C_{60}$ measured at 9.6 GHz (left panel) and 51.6 GHz (right panel).

## RESULTS AND DISCUSSION

Figure 1 shows the temperature dependence of the integrated EPR spectra of $(CH_3NH_2)K_3C_{60}$ measured at $\nu_L=9.6$ GHz (*X* band) and $\nu_L=51.6$ GHz in the vicinity of the ordering temperature, $T_N=11$ K. In the *X*-band experiments, the paramagnetic resonance signal rapidly disappears below

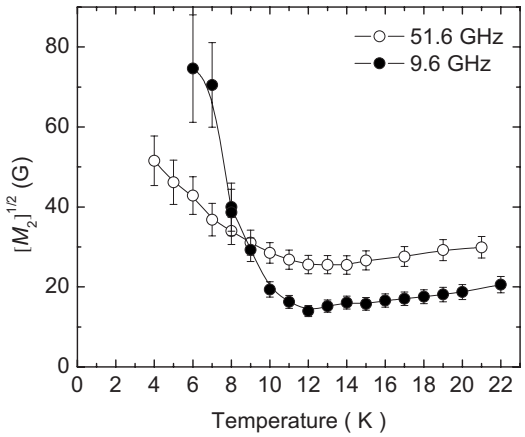


FIG. 2. Comparison of the temperature dependence of the linewidth measured at 9.6 GHz (solid circles) and 51.6 GHz (open circles) in $(CH_3NH_2)K_3C_{60}$ powder.

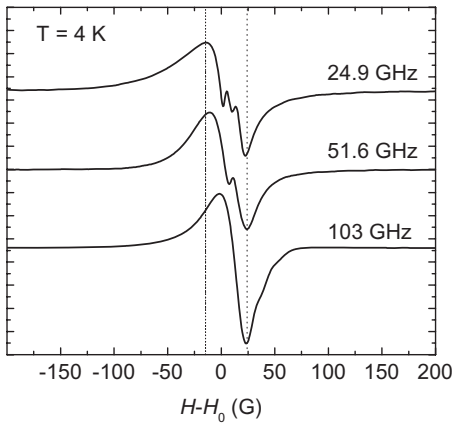


FIG. 3. EPR spectra measured at $T=4$ K and at resonance frequencies of 24.9, 51.6, and 103 GHz. The dotted vertical lines are guides to the eyes to show the linewidth reduction with increasing resonance frequency. The defect impurity line has been subtracted from the raw data.

$T_N$ in agreement with our earlier results.[12] However, close inspection of the spectra reveals that this behavior is also accompanied by the appearance of a new signal on the low-field side of the paramagnetic resonance. This low-temperature signal rapidly shifts to lower fields and simultaneously broadens with further decrease in temperature. In fact, below 6 K, it becomes so broad that a regular spectrum cannot be obtained from the derivative. In contrast to the results of the $X$-band EPR experiments, the spectra at $\nu_L = 51.6$ GHz show a less dramatic evolution with temperature. The signal now shifts only slightly on cooling below $T_N$, while the accompanying broadening effects are considerably less severe. The main resonance below $T_N$ thus behaves quite peculiarly for a normal paramagnetic resonance: the signal anisotropy, the resonance shift, and the broadening decrease with increasing frequency from 9.6 to 51.6 GHz, in sharp contrast to what is expected for a paramagnet. Such response of the EPR spectra to change in frequency is the first tentative evidence that we may be observing the emergence of an AFMR mode below 11 K.

Figure 2 shows the change in the linewidth of the EPR signal of $(CH_3NH_2)K_3C_{60}$ on cooling for the two selected resonance frequencies, 9.6 and 51.6 GHz. In order to take into account the line shape anisotropy, we use the square root of the second moment $\sqrt{M_2}$ as a measure of the linewidth. For both frequencies, the observed trend in the temperature response of $\sqrt{M_2}$ is qualitatively similar. For the paramagnetic phase, $\sqrt{M_2}$ first decreases with decreasing temperature reaching a minimum just above $T_N$. In addition, $\sqrt{M_2}$ is larger at the higher frequency (or larger resonance field). This result directly extrapolates from and is in agreement with the behavior observed in our earlier data[12] at low resonance frequencies between 209 MHz and 9.6 GHz. The origin of this frequency-dependent change in the linewidth was attributed to the presence of $g$-factor anisotropy, which rapidly increases below 200 K in the paramagnetic state. Below $T_N$, the signal suddenly broadens for both frequency measurements as a result of the emergence of local magnetic fields. The linewidth parameter is thus very sensitive to the magnetic ordering and, as will be discussed later, it measures the order parameter in the magnetically ordered state. In addition, the trend in the linewidth dependence on resonance frequency is reversed below $T_N$. The temperature-induced broadening is less pronounced at the higher frequency and for temperatures below ~8 K, the linewidth determined at 51.6 GHz is even smaller than that at 9.6 GHz (Fig. 2). Unfortunately, as commonly observed for powdered samples, the low-temperature $X$-band signal becomes so broad below 6 K that it is not possible to follow the trend to even lower temperatures.

The reciprocal dependence of the linewidth on resonance frequency in powdered samples is indicative of the emergence of an AFMR mode.[17–20] Unambiguous experimental identification of the AFMR necessitates EPR measurements at magnetic fields larger than the spin-flop field whereupon Eq. (2) is obeyed. In order to address this issue, we performed additional detailed frequency-dependent measurements at several selected temperatures below and above $T_N$. Figure 3 shows a comparison of the EPR spectra of $(CH_3NH_2)K_3C_{60}$ at 4 K (well below $T_N$) in the frequency range between 24.9 and 103 GHz. Recalling that paramagnetic contribution to the EPR signal is negligible at this temperature,[12] it is immediately apparent that the AFMR line becomes narrower with increasing frequency. At still larger resonance fields (spectra not shown here), the signal starts to broaden again. The change in the extracted linewidth at temperatures of 4, 8, and 25 K is shown in Fig. 4 as the frequency is increased to 420 GHz. At $T=25$ K, $\sqrt{M_2}$ varies linearly with frequency (dotted line in Fig. 4) as expected for a paramagnetic system. The $g$-factor anisotropy $\delta\gamma = 750(30)$ ppm (or $\Delta g = 0.0015$) derived from the linear fit is in excellent agreement with our earlier estimates.[12] On the other hand, the behavior at temperatures below $T_N$ is drastically different. At $T=4$ K, the linewidth versus frequency data show a minimum in the frequency range between 50 and 100 GHz. In the low-frequency regime, the linewidth decreases rapidly as $\nu_L$ increases, while at frequencies higher than 100 GHz, it increases with a rate comparable to that observed in the paramagnetic phase. The low-frequency behavior is not as pronounced when the temperature ap-

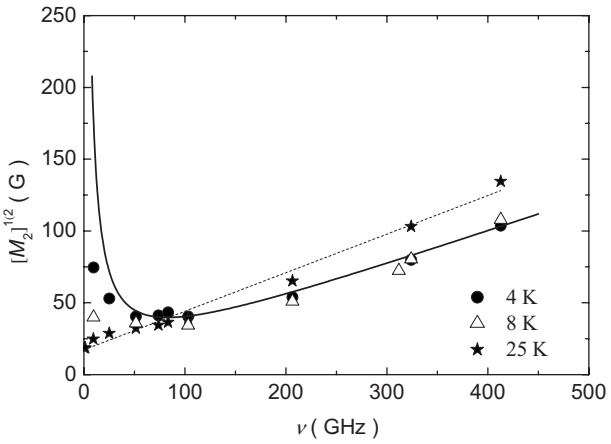


FIG. 4. Frequency dependence of the EPR linewidth measured at 4 K (solid circles), 8 K (open triangles), and 25 K (stars). The solid line is a fit of the $T=4$ K data to Eq. (2) with $\delta\gamma=710(50)$ ppm and $H_{sf}=840(80)$ G, while the dotted line is a linear fit of the $T=25$ K data with $\delta\gamma=750(30)$ ppm.

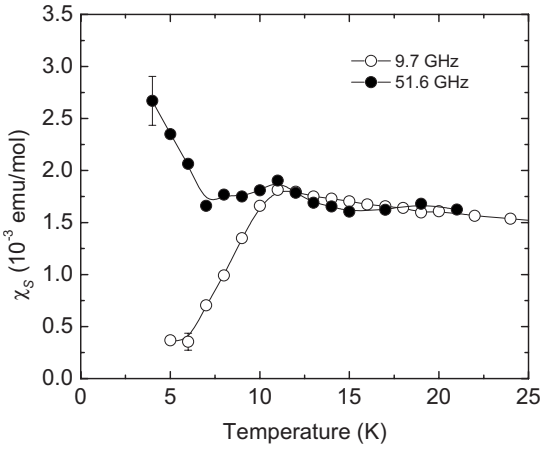


FIG. 5. Temperature dependence of the paramagnetic resonance signal intensity (open circles, determined from the *X*-band EPR data) is compared with the intensity of the 51.6 GHz data (solid circles), which is below $T_N=11$ K related to the perpendicular susceptibility $\chi_\perp$ given by the antiferromagnetic resonance signal intensity (see text for details).

proaches $T_N$ from below ($T=8$ K), though the same trend is qualitatively evident. Fitting the frequency dependence of the linewidth at $T=4$ K to Eq. (2) leads to a satisfactory agreement with experiment. The spin-flop field is found to be $H_{sf}=840(90)$ G, while the obtained *g*-factor anisotropy $\delta\gamma=710(50)$ ppm is comparable to that determined at 25 K. The small reduction in anisotropy on cooling is in agreement with the trend established in our earlier low-frequency EPR experiments.[12] Using directly the expression for the second moment, which for $(\omega/\gamma)\gg H_{sf}$ reads as $M_2=\frac{12}{175}[H_{sf}^4/(\omega/\gamma)^2]$,[18] we obtained a slightly higher spin-flop field $H_{sf}=1005(50)$ G. The small numerical difference in the spin-flop field values obtained by the two methods is believed to arise from the difficulties in the calculation of the second moment of the broad and anisotropic AFMR lines. Nevertheless, the above analysis gives the limits for the spin-flop field to be between 840 and 1000 G. The multifrequency linewidth analysis of the resonance signal below $T_N$ thus unambiguously confirms its assignment to an AFMR mode, thereby authenticating the occurrence of long-range AFM ordering below 11 K in $(CH_3NH_2)K_3C_{60}$.

The *X*-band EPR-derived spin susceptibility of the paramagnetic signal $\chi_s$ rapidly decreases over a few degrees below $T_N$ (Fig. 5). This drop in $\chi_s$ does not imply that the spin susceptibility really vanishes in the powdered sample but rather that the resonance signal at 9.6 GHz becomes unobservable at the lowest temperature because of the accompanying large broadening. Instead, in the antiferromagnetic state and for resonance fields larger than the spin-flop field, the resonance signal intensity measures the perpendicular magnetic susceptibility, $\chi_\perp=N_A\mu_{eff}^2/6k_BT_N$, where $N_A$ is the Avogadro constant and $k_B$ the Boltzmann constant.[19] While the intensity of the paramagnetic resonance signal found in *X*-band EPR measurements rapidly disappears below $T_N$,[12] the intensity of the resonance signal measured at 51.6 GHz does not change substantially on going through the Néel temperature (Fig. 5) and only a small anomaly is evident at 11 K. Below 6 K, the signal intensity starts to gradually increase and approaches a value of $\chi_\perp\approx 2.5(3)\times 10^{-3}$ emu/mol at 4 K. We stress here that the intensity of the surviving paramagnetic signal still visible at this temperature corresponds to less than 1% of the magnitude of $\chi_\perp$. Taking the extracted value of $\chi_\perp$ as an average low-temperature spin susceptibility, we can estimate the ordered magnetic moment to be $\mu_{eff}=0.7(1)\mu_B/C_{60}$. The ordered moment is comparable to that determined for the $(NH_3)K_3C_{60}$ fulleride ($\mu_{eff}=0.9\mu_B/C_{60}$).[19] Of particular interest is also the observation of a gradual increase in $\chi_\perp$ below 6 K, i.e., deep in the antiferromagnetic phase. We note that a similar anomaly has been also found in the $(TDAE)C_{60}$ ferromagnet where it has been ascribed to the low-temperature orbital ordering of Jahn-Teller distorted $C_{60}^-$ ions.[21–23] It is intriguing to consider that an analogous process may be also taking place in $(CH_3NH_2)K_3C_{60}$, thereby accounting for the slightly reduced magnitude of the magnetic moment in comparison with the ammoniated system and for the residual temperature dependence of $\chi_\perp$ below $T_N$. Direct evidence for the occurrence of such low-temperature dynamics of the $C_{60}^{3-}$ orbital ordering in $(CH_3NH_2)K_3C_{60}$ will have to await additional temperature-dependent $^{13}C$ NMR experiments.

The experimental findings thus far—observation of a decreasing linewidth and field shift with increasing EPR frequency and nondisappearance of the resonance signal—have provided compelling evidence of the emergence of an AFMR mode at temperatures below 11 K in $(CH_3NH_2)K_3C_{60}$. Under these circumstances, the temperature dependence of the AFMR linewidth, which reflects the temperature dependence of the anisotropy field, $H_A$ also provides a direct measurement of the evolution of the sublattice magnetization. In molecular systems such as the fulleride salts, the anisotropy field originates from dipolar fields[24] and one can therefore write $M\propto\sqrt{H_EH_A}$. In the high temperature expansion limit, the square of the sublattice magnetization thus becomes proportional to the linewidth: $M^2\propto\Delta H$. Figure 6 shows the temperature evolution of the square root of the normalized

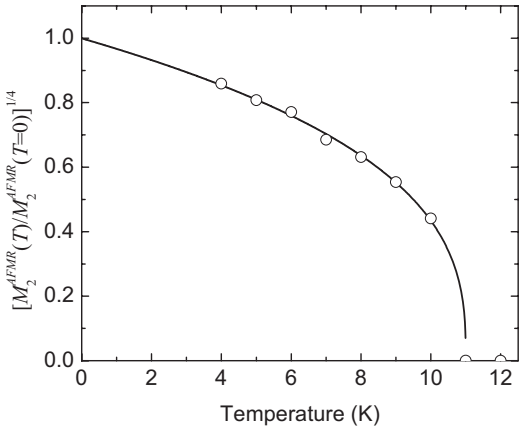


FIG. 6. Temperature dependence of the normalized $[M_2^{AFMR}(T)/M_2^{AFMR}(T=0\ \mathrm{K})]^{1/4}$ parameter, which is a measure of the sublattice magnetization $M$ obtained from the high-frequency EPR experiments at $\nu_L=51.6$ GHz. The solid line is a fit of the data to a critical law $\left[\frac{(T_N-T)}{T_N}\right]^{\beta}$ with $T_N=11$ K (fixed) and $\beta=0.35(1)$.

AFMR linewidth parameter, $[M_2^{AFMR}(T)/M_2^{AFMR}(T=0\ \mathrm{K})]^{1/4}$, where $M_2^{AFMR}(T)=M_2(T)-M_2(T=11\ \mathrm{K})$ is the increase in the second moment in the antiferromagnetic state. The observed variation can be described by the critical law $(T_N-T/T_N)^{\beta}$ with $T_N=11$ K (fixed) and $\beta=0.35(1)$. The critical exponent $\beta$ is close to what is expected for a three-dimensional Heisenberg antiferromagnet ($\beta=0.367$) and in excellent agreement with the value, $\beta=0.39(6)$, obtained by ZF-$\mu^+$SR experiments.[11]

A remaining important question to address concerns the magnitude of the AFM ordering temperature in $(CH_3NH_2)K_3C_{60}$. The observed $T_N$ of 11 K is drastically reduced when compared to the values encountered in the related ammoniated alkali fulleride family, $(NH_3)K_{3-x}Rb_xC_{60}$.[25,26] Given that the unit cell volume of $(CH_3NH_2)K_3C_{60}$ is comparable to that of $(NH_3)KRb_2C_{60}$ (Table I), one expects comparable widths of the $t_{1u}$-derived band in these two systems and therefore comparable magnitudes of the antiferromagnetic exchange interactions between neighboring fulleride ions and a $T_N$ value for $(CH_3NH_2)K_3C_{60}$ on the order of 70–80 K. Disorder effects have been detected by ZF-$\mu^+$SR experiments for both systems as a distribution of the local static magnetic fields sensed by the muon probe.[7,11,25] In particular, the distributions of the local fields, $\langle \Delta B^2 \rangle^{1/2}$, in the AFM state are 25 and 31 G in $(NH_3)K_3C_{60}$ and $(NH_3)Rb_3C_{60}$, respectively, and 13 G in $(CH_3NH_2)K_3C_{60}$. We thus conclude that disorder effects cannot alone explain the reduced $T_N$ in the methylaminated fulleride, as the field distribution is at least as sharp as in the ammoniated materials. At the same time, both $(NH_3)K_{3-x}Rb_xC_{60}$ and $(CH_3NH_2)K_3C_{60}$ have related orthorhombic crystal structures and frustration effects can also be excluded. On the other hand, we note that the present high-field EPR experiments allowed us to extract a value of the spin-flop field in $(CH_3NH_2)K_3C_{60}$, which is in the range $H_{sf}=840-1000$ G and is significantly smaller than that reported for $(NH_3)K_3C_{60}$ ($H_{sf}=1700$ G, $T_N=40$ K).[18] Since the anisotropy field $H_A$ in the antiferromagnetic fullerides principally arises from dipolar contributions, it is unlikely that it changes significantly on going from $(NH_3)K_3C_{60}$ to $(CH_3NH_2)K_3C_{60}$. Therefore, the reduced magnitude of $H_{sf}$ in $(CH_3NH_2)K_3C_{60}$ should reflect a reduction in the interfulleride exchange interactions. Since the exchange field $H_E$ is directly proportional to the exchange coupling constant $J$, it should also roughly scale with $T_N$. One thus expects that the spin-flop fields in the two systems will scale with $\sqrt{T_N}$, which is in agreement with the observed experimental trend. Therefore, while $(CH_3NH_2)K_3C_{60}$ also orders antiferromagnetically, the interfulleride exchange interactions are anomalously weak. The origin of this effect may derive from the increased orthorhombic anisotropy in $(CH_3NH_2)K_3C_{60}$ that is driven by the elongated $CH_3NH_2$ cointercalant.

TABLE I. Lattice parameters, unit cell volume, long and short $C_{60}$-$C_{60}$ nearest contacts, anisotropy ratio ($R_{long}/R_{short}$), and Néel temperature for the orthorhombic $(NH_3)K_3C_{60}$, $(NH_3)KRb_2C_{60}$, and $(CH_3NH_2)K_3C_{60}$ fullerides at room temperature.

| | $(NH_3)K_3C_{60}$ | $(NH_3)KRb_2C_{60}$ | $(CH_3NH_2)K_3C_{60}$ |
|---|---|---|---|
| $a$ (Å) | 14.971 | 15.100 | 15.203 |
| $b$ (Å) | 14.917 | 15.006 | 15.180 |
| $c$ (Å) | 13.692 | 13.766 | 13.503 |
| $V$ (Å$^3$) | 764.4 | 782.4 | 779.1 |
| Long $R_{C_{60}\text{-}C_{60}}$ (Å) | 10.567 | 10.662 | 10.742 |
| Short $R_{C_{60}\text{-}C_{60}}$ (Å) | 10.134 | 10.209 | 10.163 |
| Anisotropy ratio | 1.043 | 1.044 | 1.057 |
| $T_N$ (K) | 40 | 76 | 11 |

Table I compares the room temperature lattice parameters and near neighbor $C_{60}$-$C_{60}$ distances for both ammoniated and methylaminated samples.[10,24,27] Clearly, the expansion of the parent $A_3C_{60}$ fulleride structure upon intercalation of ammonia and methylamine is significantly more anisotropic in the case of $(CH_3NH_2)K_3C_{60}$. The enhanced anisotropy should presumably affect the splitting between the $t_{1u}$ orbitals as well as their overlap and thus alter the exchange interaction between neighboring $C_{60}^{3-}$ ions. The structural anisotropy thus inevitably introduces also anisotropy in the exchange pathways. Although the $(CH_3NH_2)K_3C_{60}$ is still essentially three dimensional and in these terms comparable to the other fulleride phases, the three dimensional antiferromagnetic transition temperature becomes a function of anisotropy in $J$. In this respect, the suggested transition from the dynamic to static Jahn-Teller distortion below 6 K may further facilitate the anisotropy in $J$ and introduce exchange anisotropies, such as the Dzyaloshinsky-Moriya interaction, for instance, and it may also explain the residual temperature dependence of the susceptibility below $T_N$. At the same time, as the methyl groups approach very closely the fullerene molecules,[10] the ensuing fullerene-H-C interactions could affect the type and/or degree of orbital ordering of the $C_{60}^{3-}$ units, thereby indirectly controlling the exchange pathways between fullerene magnetic moments.

## CONCLUSIONS

In conclusion, we have detected the emergence of the antiferromagnetic resonance mode in powdered

$(CH_3NH_2)K_3C_{60}$ by detailed temperature- and frequency-dependent magnetic resonance measurements below $T_N=11$ K. The characteristic "anomalous" linewidth dependence between 9.6 and 103 GHz, where the signal linewidth decreases with increasing resonance frequency, is taken as firm evidence for AFMR and enables us to estimate the spin-flop field in the range $H_{sf}=840-1000$ G. The ordered magnetic moment, calculated from the low-temperature spin susceptibility $\chi_\perp$, is estimated to be $\mu_{eff}=0.7(1)\mu_B/C_{60}$. The dramatic reduction in the Néel temperature and in the spin-flop field when compared to the ammoniated fulleride analogs at comparable interfullerene separations reveal a drastic weakening of the near neighbor $C_{60}^{3-}$-$C_{60}^{3-}$ exchange constants in $(CH_3NH_2)K_3C_{60}$. Such an effect may be related to the influence on the electronic properties of the pronounced enhancement of the anisotropy in the expanded unit cell of the methylaminated salt promoted by the anisotropic shape of the cointercalant.

## ACKNOWLEDGMENTS

We thank the EPSRC for financial support (M.J.R. and K.P.) and the NHMFL for access to the high-field magnetic resonance facilities.

[1] E. Koch, O. Gunnarsson, and R. M. Martin, Phys. Rev. Lett. **83**, 620 (1999).
[2] O. Gunnarsson, *Alkali-Doped Fullerides* (World Scientific, Singapore, 2004).
[3] R. M. Fleming, A. P. Ramirez, M. J. Rosseinsky, D. W. Murphy, R. C. Haddon, S. M. Zahurak, and A. V. Makhija, Nature (London) **352**, 787 (1991).
[4] P. Durand, G. R. Darling, Y. Dubitsky, A. Zaopo, and M. J. Rosseinsky, Nat. Mater. **2**, 605 (2003).
[5] K. M. Allen, S. J. Heyes, and M. J. Rosseinsky, J. Mater. Chem. **6**, 1445 (1996).
[6] Y. Iwasa, H. Shimoda, T. T. M. Palstra, Y. Maniwa, O. Zhou, and T. Mitani, Phys. Rev. B **53**, R8836 (1996).
[7] K. Prassides, S. Margadonna, D. Arcon, A. Lappas, H. Shimoda, and Y. Iwasa, J. Am. Chem. Soc. **121**, 11227 (1999).
[8] S. Margadonna and K. Prassides, J. Solid State Chem. **168**, 639 (2002).
[9] O. Zhou, T. T. M. Palstra, Y. Iwasa, R. M. Fleming, A. F. Hebard, P. E. Sulewski, D. W. Murphy, and B. R. Zegarski, Phys. Rev. B **52**, 483 (1995).
[10] A. Y. Ganin, Y. Takabayashi, C. A. Bridges, Y. Z. Khimyak, S. Margadonna, K. Prassides, and M. J. Rosseinsky, J. Am. Chem. Soc. **128**, 14784 (2006).
[11] Y. Takabayashi, A. Yu. Ganin, M. J. Rosseinsky, and K. Prassides, Chem. Commun. (Cambridge) **2007**, 870 (2007).
[12] A. Y. Ganin, Y. Takabayashi, M. Pregelj, A. Zorko, D. Arčon, M. J. Rosseinsky, and K. Prassides, Chem. Mater. **19**, 3177 (2007).
[13] A. K. Hassan, L. A. Pardi, J. Krzystek, A. Sienkiewicz, P. Goy, M. Rohrer, and L. C. Brunel, J. Magn. Magn. Mater. **142**, 300 (2000).
[14] J. van Tol, L. C. Brunel, and R. J. Wylde, Rev. Sci. Instrum. **76**, 074101 (2005).
[15] See, for instance A. Abragam, *Principles of Nuclear Magnetism* (Oxford University Press, Oxford, 1986), p. 107.
[16] K. Yosida, Prog. Theor. Phys. **7**, 425 (1952).
[17] A. Janossy, N. Nemes, T. Feher, G. Oszlanyi, G. Baumgartner, and L. Forro, Phys. Rev. Lett. **79**, 2718 (1997).
[18] M. Bennati, R. G. Griffin, S. Knorr, A. Grupp, and M. Mehring, Phys. Rev. B **58**, 15603 (1998).
[19] F. Simon, A. Janossy, F. Muranyi, T. Feher, H. Shimoda, Y. Iwasa, and L. Forro, Phys. Rev. B **61**, R3826 (2000).
[20] D. Arčon, K. Prassides, A. L. Maniero, and L. C. Brunel, Phys. Rev. Lett. **84**, 562 (2000).
[21] R. Blinc, P. Jeglič, T. Apih, J. Seliger, D. Arčon, and A. Omerzu, Phys. Rev. Lett. **88**, 086402 (2002).
[22] P. Jeglič, R. Blinc, T. Apih, A. Omerzu, and D. Arčon, Phys. Rev. B **68**, 184422 (2003).
[23] D. Arčon, P. Jeglič, T. Apih, A. Omerzu, and R. Blinc, Carbon **42**, 1175 (2004).
[24] J. B. Torrance, H. J. Pedersen, and K. Bechgaard, Phys. Rev. Lett. **49**, 881 (1982).
[25] T. Takenobu, T. Muro, Y. Iwasa, and T. Mitani, Phys. Rev. Lett. **85**, 381 (2000).
[26] J. Arvanitidis, K. Papagelis, T. Takenobu, I. Margiolaki, K. Brigatti, K. Prassides, Y. Iwasa, and A. Lappas, Physica B **326**, 572 (2003).
[27] S. Margadonna, K. Prassides, H. Shimoda, T. Takenobu, and Y. Iwasa, Phys. Rev. B **64**, 132414 (2001).